Scientific Papers. Series A. Agronomy, Vol. LXVIII, No. 2, 2025
ISSN 2285-5785; ISSN CD-ROM 2285-5793; ISSN Online 2285-5807; ISSN-L 2285-5785

CHARACTERISATION OF PEDOGENIC CARBONATES IN CALCOCAMBISOL AT A LOCATION IN THE DINARIC PART OF CROATIA

Katarina MATAN[1], Aleksandra BENSA[1], David DOMÍNGUEZ-VILLAR[2], Mirna ŠVOB[1], Kristina KRKLEC[1, 2]

[1]University of Zagreb, Faculty of Agriculture, Svetošimunska cesta 25, 10000, Zagreb, Croatia
[2]University of Salamanca, Plaza de los Caídos s/n, 37008, Salamanca, Spain

Corresponding author email: kmatan@agr.hr

Abstract

Pedogenic carbonates are secondary carbonate deposits and are a constitutional part of many soils. We analysed a 95 cm deep Calcocambisol soil profile at a location in the Dinaric part of Croatia. Here, pedogenic carbonates are more abundant in the deeper part of the profile (>23 cm), and their amount and size increase with depth corresponding to soil properties along the profile. These pedogenic carbonates are spherical to irregular in shape and can be classified as nodules. Microscopical analysis of these nodules shows that dissolution and re-precipitation of carbonate take place in situ, without considerable movement through the soil profile. The growth of the nodules starts from multiple centres of nucleation, and their internal structure is a result of spatial and temporal environmental conditions in the soil matrix during carbonate precipitation. The inclusion of noncarbonate particles and preservation of the original soil structure confirm the replacive nature of nodule growth. Furthermore, the internal structure of nodules reveals multiple stages of calcite precipitation, indicating seasonal or event-based precipitation of carbonate.

Key words*: pedogenic carbonates, calcite nodules, Calcocambisol, Croatia, Dinarides.*

INTRODUCTION

Pedogenic carbonates (PC) are secondary carbonate precipitates in soils and are most commonly a result of chemical weathering processes of carbonate rocks. They are a constitutional part of many soils (West et al., 1988; Chesworth, 2008), with a direct impact on the soils hydraulic properties (Castellini et al., 2019) and erodibility (Panagos et al., 2014), and have a high potential of carbon sequestration (Egli et al., 2021).

The formation of PC depends on different abiotic and biotic factors but is predominantly controlled by environmental factors temperature and the amount of precipitation (Borchardt & Lienkaemper, 1999), as well as soil moisture and carbon dioxide concentration. PC can be formed in a wide range of climates (Amit et al., 2011) but are more characteristic for soils in areas with higher temperatures where evapotranspiration exceeds precipitation (Royer, 1999). Thus, PC are commonly found in many soils in Mediterranean climates (Jiménez-Ballesta et al., 2023), such as Terra rosa (Domínguez-Villar et al., 2022), Calcic luvisols (Rovira & Vallejo, 2008), Cambisols and Regosols (Jiménez-Ballesta et al., 2023).

Pedogenic carbonates are formed in soils from geogenic (i.e. from soil parent material or allogenic particles), biogenic (i.e. from carbonates formed within or released by animals and plants), or older PC (Zamanian et al., 2016). They differ in morphology, shape, size, density, porosity and amount of incorporated impurities. Thus, according to the size of the carbonate crystals forming them, PC can be classified as micrite (<5 μm-long carbonate crystals), microsparite (between 5 and 20 μm long), and sparite (>20 μm long) (Becze-Deàk et al., 1997). As well, PC can form different morphologies, such as: earthworm biospherolits, rhizoliths, hypocoatings (pseudomycels), nodules, coatings on clasts, calcretes, and laminar caps (Zamanian et al., 2016).

Studies of PC have been conducted worldwide, especially in carbonate areas (e.g. Cerling & Bowman, 1989; Driese & Mora, 1993; Naiman et al., 2000; Wagner et al., 2012; Jiménez-Ballesta et al., 2023; Bayat et al., 2023; Fu et al., 2024), but there is still a limited number of

studies on this topic done in Dinaric karst area (Brlek & Glumac, 2014; Bensa et al., 2021; Domínguez-Villar et al., 2022).

Calcocambisol is one of the most common soil types developed over carbonates in Dinaric karst area (Pilaš et al., 2016; Hasan et al., 2020). Here, Calcocambisols mainly form by weathering and transformation processes observed in carbonate rocks of different ages (Škorić et al., 1985; Husnjak, 2014). Furthermore, Calcocambisol formation is as well influenced by relief characteristics, resulting in its high spatial variability (Vrbek & Pilaš, 2007a; 2007b) and resulting in the development of soils of various depths (Bogunović et al., 2009).

Calcocambisols are silty clayey to clayey soils having favourable soil-water relations due to stable granular and angular structure (Husnjak, 2014; Švob et al., 2021). Furthermore, it has an acidic (Škorić et al., 1985; Miloš & Maleš, 1998) to an alkaline reaction (Bogunović et al., 2009; Miloš & Bensa, 2014) depending on the presence of the carbonates. The production potential of these soils varies and is influenced by numerous factors, including rockiness, skelet content, slope, elevation, and soil depth. If present in the soil, PC can present a problem, affecting soil properties and potentially impacting plant growth.

North Dalmatian Plain is a vast levelled carbonate surface located in the Dinaric karst region (Figure 1). It is dominantly built up by carbonate Upper Cretaceous to the Oligocene lithologies intercalated with marly sediments and occasional bauxites and coal beds (Mamužić, 1971; Ivanović et al., 1978; Velić and Vlahović, 2009). Here, Calcocambisols are a common soil type (Čolak & Martinović, 1973), occasionally characterized by the presence of PC within the soil profile. Thus, the aim of this study is to characterize PC developed in Calcocambisol soil profile at a location within the North Dalmatian Plain.

MATERIALS AND METHODS

The study site (43°47'39" N, 16°00'08" E; 200 m asl) is located in the southeast part of the North Dalmatian Plain (Croatia) within the southern part of Krka National Park (Figure 1 A). The carbonate bedrock at the study site is composed of Eocene foraminiferal limestones and carbonate conglomerates (i.e. Promina Beds) (Ivanović et al., 1977; Brlek et al., 2014), intensively faulted and folded forming structures having Dinaric orientation (i.e., NW-SE) (Figure 1 B). Study site is characterised by discontinuous Calcocambisol soil, typically up to < 0.3 meter thick, with rock exposures covering up to 50% of the terrain (Švob et al., 2021; Bensa et al., 2021). Although, regionally Calcocambisols form shallow soil cover (Vrbek & Pilaš, 2007a), locally in areas where rock fissures occur (as a result of the karstification process) soil depth may extend up to 1 meter (Bogunović et al., 2009; Švob et al., 2021). The study area is characterized by a Mediterranean (Csa) type of climate with dry and hot summers and mild, rainy winters (Filipčić, 1998), and local meteorological conditions are being recorded since 2019 in a station installed in a proximity of study site. Here the mean annual temperature during 2019-2023 period was 14.9°C, while the annual amount of precipitation during this period was 1060 mm with both having clear seasonal pattern.

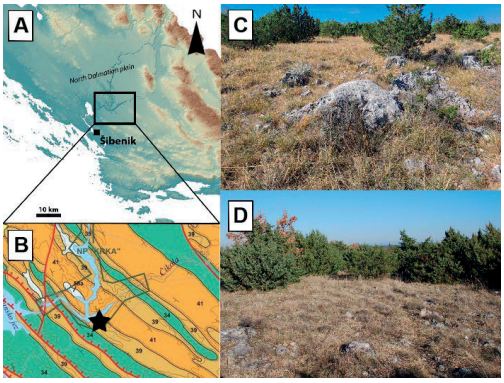

Figure 1. Location of the studied site: A. Location of the study site in the Adriatic part of Croatia; B. Geological map of the study area (after CGI, 2009); 58a: Quaternary sediments, 41: Eocene-Oligocene detrital carbonates (including conglomerates) 39: Eocene foraminiferal limestones, 34: Cretaceous limestones; C. and D. Natural vegetation and soil cover at study site

Vegetation of study site is characterised by fragmented evergreen oak (Quercus ilex) and flowering ash forest (Fraxino orni-Quercetum ilicis H-ić/1956/1958) (Medak & Perić, 2007) degraded to the garrigue state (Figure 1 C, 1 D). Due to reduced amount of biomass production, this type of vegetation has a

minimum impact on soil morphology (Vrbek & Pilaš, 2007a).

To investigate soil properties, a 95 cm deep soil profile was dug out and soil sampling was performed along vertical axis of the profile, at 5 cm intervals. Sampling comprised of collection of soil samples in a non-disturbed state using 100 cm3 cylinders, as well as of collection of bulk soil samples. Soil properties were investigated and described following FAO recommendations (2006). Field capacity (FC) was determined by the gravimetric method with core samples, (ISO 11461:2001). Subsequently, the same samples were used for gravimetric determination of bulk density (BD) post-drying at 105°C, adhering to the methods (ISO 11272:2017). According to ISO 11508:2017, the particle density (PD) was measured in water using a 100-mL pycnometer, and according to Danielson & Sutherland (1986), total porosity (TP) and air porosity (AP) were calculated.

Bulk soil samples were air-dried, followed by separation of carbonate particles (i.e. skelet and pedogenic particles), while the rest of the sample was ground and sieved using a sieve with a 2 mm mesh size (ISO 11464:2006). Particle size distribution analysis was done using the pipette method, with wet sieving and sedimentation after dispersion with sodium-pyrophosphate (Na4P2O7, c = 0.4 M) (ISO 11277:2009).

Soil pH values were measured using a combined glass electrode in a 1:5 (v/v) suspension of soil in water and soil in KCl solution (c=1M) according to ISO 10390:2005. The humus content was analyzed by acid potassium-dichromate (K2Cr2O7, c=0.4M) digestion, following the method of Tjurin (JDPZ, 1966), and soil organic carbon (SOC) content was calculated by dividing the content of humus by 1.724 (the Van Bemmelen factor). Total carbonate content was determined by applying the modified volumetric method (ISO 10693:1995). All soil analyses were performed in the Laboratory of the Department of Soil Science, at the Faculty of Agriculture, University of Zagreb.

The analysis of PC within soil samples comprised of particle classification, morphometry, and microscopic analyses. PC were examined using binocular lenses, polarizing petrographic microscope and Scanning Electron Microscope (SEM) at CENIEH (Burgos, Spain). Thus, in order to eliminate the surrounding clay, PC were briefly rinsed in tap water (using an ultrasonic bath). Those to be inspected using SEM were dried overnight in an oven at 50 ˚C and let to cool down in a desiccator until they were gold coated before their analysis, while others were embedded in epoxy resin before being cut and mounted in thin sections to be observed using a polarizing petrographic microscope.

RESULTS AND DISCUSSIONS

The studied soil profile consists of the following mineral horizons: A-Bw-Bk-R (Figure 2). The A horizon (0-7 cm) is characterized by dark brown colour (7.5 YR 4/4) indicating organic matter accumulation. It features a granular structure and common plant roots. The underlying cambic Bw horizon (7-23 cm) is reddish brown (5 YR 4/4) characterized by the increased clay content, noticed by the feel. It has an angular blocky structure and very few to few plant roots. The Bk horizon (23-95 cm) is characterized by the accumulation of PC, mostly in the form of nodules. Furthermore, rock fragments ranging in size from fine gravel (2-6 mm) to gravel (6-20 mm) also occur, Figure 2. Their abundance can be classified as many (15-40%) according to FAO (2006). The R horizon at the bottom of the soil profile refers to the hard, non-weathered rock underlying the soil profile - parent material.

Bulk density (BD) values of the studied soil increased with depth from 1.11 g cm^{-3} to 1.67 g cm^{-3} (Table 1). The lowest BD value was measured in topsoil (0-5 cm) and can be attributed to the highest SOC content of 4.70% (Table 3) and granular structure (Hakånsson & Lipiec, 2000). The increase of BD values with depth suggests soil compaction occurring in the Bw and Bk horizons, which implies restrictions in water movement and root growth. This compaction is linked to higher clay content and an angular blocky structure (FAO, 2006). Particle density (PD) values varied across the profile (2.44-2.62 g cm^{-3}), Table 1, with the lowest values measured within the first 10 cm of depth. The individual values of PD point to differences in SOC content and mineralogy (Hollis et al., 2012).

The highest field capacity (FC) values (42.70% and 41.75%; Table 1), were measured in topsoil horizon (up to a depth of 10 cm) and can be attributed to the accumulation of humified organic matter (Bensa et al., 2021). Across the soil profile, the average FC value was 35.02%, while the lowest values were measured in the deeper parts of the profile (28.86% at 75-80 cm and 29.13% at 50-55 cm depth). These low values can be attributed to the high content of sand particles (Švob et al., 2021), as indicated in Table 2.

Total porosity (TP) values show variation throughout the soil profile, with an average value of 43.43%. Air capacity (AC) values also varied across the soil profile, from 1.03% recorded at a depth of 85–90 cm to 14.03% at a depth of 10-15 cm (Table 1). Very low AC values at the bottom of the soil profile (> 70 cm) are linked to low TP values and high BD values. The measured physical properties of the studied soil are consistent with the previous findings for Calcocambisol in this area (Čolak & Martinović, 1973; Miloš & Maleš, 1998; Švob et al., 2021).

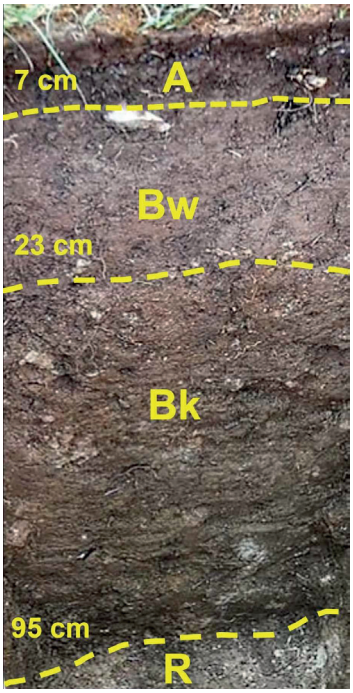

Figure 2. Studied soil profile with indicated soil horizons

Table 1. Basic physical properties of the investigated soil profile

Soil depth (cm)	Bulk density (g cm^{-3})	Particle density (g cm^{-3})	Field capacity (%)	Total porosity (%)	Air capacity (%)
0-5	1.11	2.44	42.70	54.41	11.71
5-10	1.18	2.44	41.75	51.50	9.75
10-15	1.13	2.48	40.37	54.40	14.03
15-20	1.23	2.51	39.48	51.05	11.57
20-25	1.23	2.54	39.65	51.41	11.76
25-30	1.39	2.56	33.92	45.66	11.74
30-35	1.41	2.56	35.46	44.79	9.33
35-40	1.48	2.58	33.42	42.48	9.06
40-45	1.48	2.58	33.32	42.84	9.52
45-50	1.48	2.58	32.97	42.83	9.86
50-55	1.55	2.62	29.13	40.61	11.48
55-60	1.60	2.59	30.59	38.11	7.52
60-65	1.58	2.61	31.29	39.55	8.26
65-70	1.55	2.60	32.00	40.27	8.27
70-75	1.63	2.58	34.88	36.88	2.00
75-80	1.67	2.60	28.86	35.79	6.93
80-85	1.66	2.57	31.73	35.53	3.80
85-90	1.58	2.56	37.43	38.46	1.03
90-95	1.58	2.57	36.35	38.56	2.21

Results of particle size distribution analysis (Table 2) show that clay particles are the most abundant soil fraction throughout the entire soil profile, having the highest values in the Bw horizon (5-30 cm). The average clay content throughout the profile is 48.3%. This is followed by the silt fraction, with an average value of 35.8 %, with a predominance of fine silt in the upper part of the soil profile (0-30 cm), while the coarse silt fraction dominates in the lower part of the soil profile. The sand fraction has the lowest proportion, with an

average of 18.9%, and increases with depth, especially coarse sand at the bottom of the soil profile (> 75 cm).

These data are comparable to previous results for Calcocambisols in this area (Čolak & Martinović, 1973; Miloš & Maleš, 1998; Švob et al., 2021).

Soil texture varies through the profile: silty clay in topsoil (0-5 cm), clay at depths 5-50 and 65-95 cm, and clay loam at depths 50-60 cm, affecting soil water content (Figure 3). Determined textural classes are typical for Calcocambisol (Škorić et al., 1985; Husnjak, 2014).

Table 2. Basic physical properties of the investigated soil profile

Depth (cm)	Coarse sand 2.0-0.2 mm	Fine sand 0.2-0.063 mm	Coarse silt 0.063-0.02 mm	Fine silt 0.02-0.002 mm	Clay < 0.002 mm
0-5	3.9	7.2	15.5	28.8	44.6
5-10	2.4	5.0	14.5	24.5	53.6
10-15	3.2	5.5	12.0	23.4	55.9
15-20	2.4	5.2	10.9	20.0	61.5
20-25	2.0	5.3	14.6	19.9	58.2
25-30	3.9	5.1	15.9	17.4	57.7
30-35	6.5	6.8	20.5	14.5	51.7
35-40	8.3	7.0	20.5	16.3	47.9
40-45	7.5	8.8	21.7	16.3	45.7
45-50	9.8	8.7	23.3	18.2	40.0
50-55	7.2	14.5	23.7	16.9	37.7
55-60	7.2	16.3	24.4	16.1	36.0
60-65	7.5	15.4	21.2	15.4	40.5
65-70	7.5	8.3	19.1	14.7	50.4
70-75	10.5	7.1	19.2	14.3	48.9
75-80	16.4	7.3	18.6	13.6	44.1
80-85	13.8	7.1	17.0	15.8	46.3
85-90	13.2	6.9	16.6	15.8	47.5
90-95	13.2	8.1	14.8	15.1	48.8

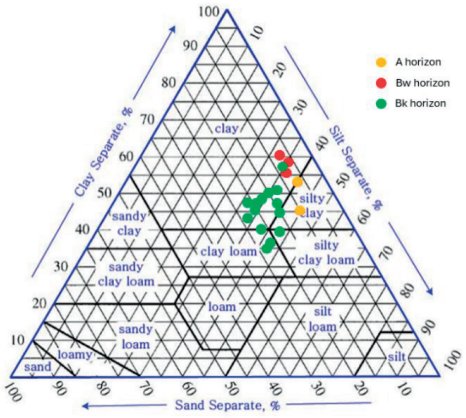

Figure 3. Distribution of soil samples on texture triangle (FAO, 2006)

The analysis of soil chemical properties reveals the lowest $pH_{(KCl)}$ values (Table 3) at the top of the soil profile that gradually increase with depth. The soil reaction is acidic in the A and Bw horizons (up to a depth of 25 cm) as a result of organic matter decomposition and the presence of humic acids, and is alkaline in the Bk horizon (> 25 cm), due to the presence of carbonates. Carbonates appear at a depth 15-20 cm (1.68%) and their amount increases with depth up to 37.38% measured at the 55-60 cm, followed by decrease up to 26.04% at the bottom of the soil profile, Table 3. The accumulation of organic matter in the topsoil (0-15 cm) leads to an increased SOC content (3.60-4.70%) reinforcing the dissolution of carbonate particles and consequently resulting in the absence of carbonates. With depth, SOC content decreases, reaching a minimum of 0.47 % at the depth of 90-95 cm (Table 2).

At the same time, pH values increase indicating that the acidic environment has been neutralized by the dissolution of carbonates, allowing the formation of PC. Measured chemical soil properties are in accordance with the results of previous studies of Calcocambisol in the area (Miloš & Maleš, 1998; Švob et al., 2021; Bensa et al., 2021).

Table 3. Chemical properties of the investigated soil profile

Soil depth (cm)	pH (H_2O)	pH (KCl)	Total carbonates (%)	SOC (%)
0-5	6.61	5.80	-	4.70
5-10	6.49	5.62	-	3.69
10-15	6.40	5.45	-	3.60
15-20	7.14	6.47	1.68	2.55
20-25	7.59	6.94	4.20	2.09
25-30	7.73	7.12	4.03	1.97
30-35	7.82	7.25	11.76	1.61
35-40	7.93	7.35	19.74	1.46
40-45	7.81	7.37	20.16	1.61
45-50	7.94	7.47	29.82	0.98
50-55	8.08	7.42	36.12	0.80
55-60	8.12	7.54	37.38	0.66
60-65	8.13	7.43	30.24	0.66
65-70	8.14	7.42	25.20	0.65
70-75	8.20	7.40	28.14	0.68
75-80	8.24	7.42	31.08	0.60
80-85	8.11	7.45	29.82	0.59
85-90	8.23	7.42	28.14	0.59
90-95	8.19	7.39	26.04	0.47

Understanding of the morphology and formation process of secondary carbonate deposits (i.e. pedogenic carbonates) is essential to address various aspects related to soil formation in arid and semiarid regions (Zamanian et al., 2016). The final morphology of these deposits is a result of the interaction of various factors: soil texture, hydrological regime, salt concentration, soil erosion, and concentration of soil CO_2 (Wieder & Yaalon, 1982; Sobecki & Wilding, 1983; Domínguez-Villar et al., 2022).

Analysis of the studied soil profile shows that PC are more abundant in the deeper part of the profile (>23 cm), and their amount and size increase with depth (Figure 2 and Table 3) corresponding to soil properties along the profile. The upper part of the soil profile (< 20 cm) is characterized by rich biological production leading to higher SOC content, and more acidic environment (i.e. lower pH values; Table 3) favouring carbonate dissolution and resulting in the absence of PC. This corresponds to "*perdescendum*" model of PC formation (Zamanian et al., 2016) where carbonate in the topsoil is dissolved, leached to the subsoil and re-precipitated; and is commonly considered to be one of the main processes of PC redistribution and accumulation in soil horizons (Machette, 1985; Royer, 1999). On the other hand, results of soil analyses showed that physical soil properties vary along the soil profile (Table 1 and Table 2), and in combination with temperature and amount of precipitation certainly affect currently active dissolution and re-precipitation of PC along the soil profile. Thus, this corresponds to *in situ* model of PC formation (Zamanian et al., 2016) where dissolution and re-precipitation of carbonate takes place without considerable movement through the soil profile and redistributes carbonates within the horizon (Monger & Adams, 1996; Rabenhorst & Wilding, 1986; West et al., 1988).

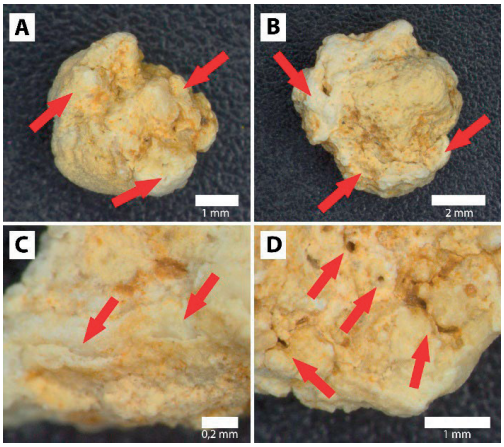

Figure 4. Pedogenic carbonate nodules from the studied soil profile analysed using binocular lenses: A. Typical semispherical calcite nodule formed by agglomeration of several nodules (indicated by red arrows); B. Irregular calcite nodule. Red arrows indicate to different constitutional parts of the nodule; C. Surface of the nodule. Red arrows indicate layers - coatings of sparite calcite attached to the nodule surface, indicating event based or seasonal carbonate accumulation due to different environmental conditions; D. Detail of pitted and hummocky nodule surface. Red arrows indicate dissolution features

Pedogenic carbonate particles from the studied soil profile are mostly spherical to irregular in shape, with diameters up to 64 mm (Figure 4), and can be classified as nodules (Barta, 2011). Nodules are commonly defined as roughly equidimensional pedofeatures that are not related to natural surfaces or voids and do not consist of single crystals (Stoops, 2003) and are usually formed *in situ* by impregnation of soil matrix with $CaCO_3$ (Durand et al., 2010), reworked to varying degrees, or inherited from

the parent material (Verrecchia & Trombino, 2021).

The majority of studied nodules from this location have sharp outer boundaries (Figure 4) and their morphology is often characterized by bulbous protrusions (Figures 4 A and 4 B) that indicate the agglomerative nature of their formation (i.e. inclusion of surrounding particles during nodule growth).

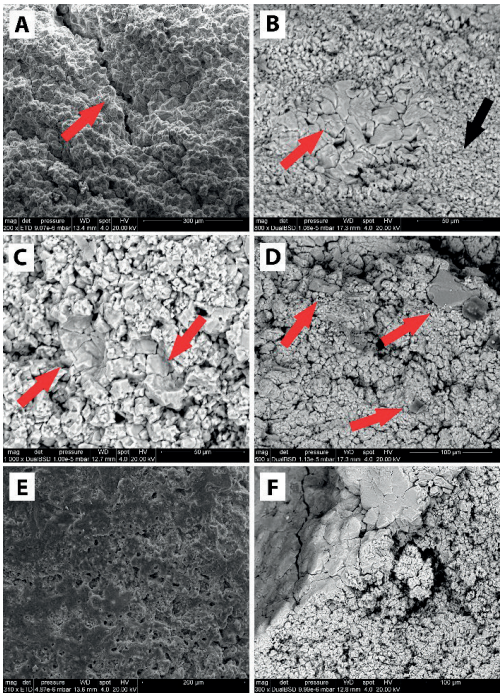

Figure 5. Pedogenic carbonate nodules from the studied soil profile analyzed using a scanning electron microscope: A. Microrunnel (i.e. dissolutional channel) on the surface of the nodule; B. Areas with micritic (black arrow) and microsparitic (red arrow) calcite; C. Casts at the surface formed by detachment of nodule components; D. Detail of the surface of carbonate nodule showing incorporated clay particles (red arrows); E. Pitted surface of the nodule indicating dissolution process; F. Edge of the carbonate nodule having surface flattened by displacive growth

Analyses of nodules using binocular lenses (Figure 4) and SEM (Figure 5) showed that surfaces of the nodules often display pitted and hummocky morphologies and features characteristic of the carbonate dissolution process. Thus, features such as dissolution pits (Figures 4 D and 5 E) and microrunnels (i.e. dissolutional channels; Figures 4 D and 5 A) are commonly observed. The carbonate dissolution process takes place not only at the surface of the nodule, but as well along voids and cavities (Krklec et al., 2013), causing the decrease of nodule cohesion and can result in detachment and removal of its components, as can be observed in Figure 5C. Furthermore, closer inspection of calcite grains surfaces reveals a lack of sharp crystal edges, reinforcing the presence of an active dissolutional process, characteristic for carbonate areas (Krklec et al., 2016; 2018; 2021; 2022; 2024).

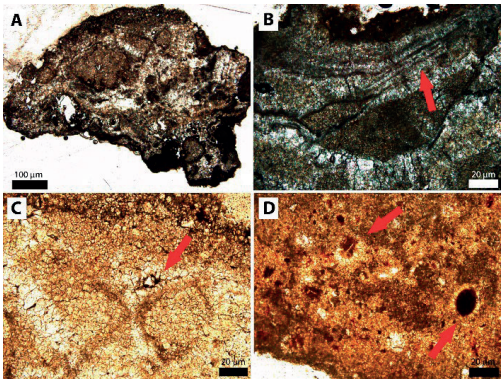

Figure 6. Pedogenic carbonate nodules from the studied soil profile analysed using polarizing petrographic microscope: A. Irregular nodule showing incorporation of various surrounding soil and carbonate particles; B. Edge of nodule showing incorporated particle with multiple stages of micrite and microsparite precipitation; C. Internal nodule structure showing the transition between micrite and microsparite calcite. Red arrow indicates larger sparite crystals formed within empty pore space; D. Detail of carbonate nodule showing the inclusion of different particles. Red arrows indicate grains surrounded by calcite that possibly served as centers of nucleation

On the other hand, analysis of nodules cross sections using polarizing petrographic microscope (Figure 6) shows internal structure of the nodules and provides additional information on carbonate precipitation and formation of these PC particles. Studied carbonate nodules are composed of calcite (micrite, microsparite and sparite) and contain inclusions of other particles (e.g., quartz crystals or soil particles). Their internal structure shows that there is no unique center of nodule nucleation, but rather carbonate precipitation starts around multiple nucleuses and progresses outwards in all directions (Figures 6 A and 6 D). The transition between

zones dominated by micrite to those dominated by microsparite is commonly gradual (Figures 6 C and 6 D), although in some cases opposite can be observed (Figures 6 A and 6 B). This distribution of micrite and microsparite crystals within nodules is a result of spatial and temporal environmental conditions in the soil matrix during carbonate precipitation. Larger sparite crystals are commonly developed in cracks or occur as larger pore infillings.

Furthermore, some nodules have features such as carbonate coatings (Figures 4 C and 6 B) where layers of micrite and microsparite interchange, usually parallel to the surface, indicating different stages of calcite precipitation. Thus, these coatings and the internal structure of nodules (interchange of micrite and microsparite) shows that studied nodules do not grow continuously but are formed in multiple stages and/or generations, indicating different pedogenetic phases (Durand et al., 2010; Verrecchia & Trombino, 2021). This episodic carbonate precipitation is driven by seasonal variations in soil moisture and CO_2 levels (Domínguez-Villar et al., 2022), highlighting the role of environmental fluctuations in nodule growth dynamics.

As previously mentioned, carbonate nodules contain inclusions of particles (e.g., quartz grains) inherited from adjacent soil matrix (Figure 5 D, 6 A and 6 D). Some of those particles serve as centres of nodules nucleation, while others are included in nodule structure during its growth. Thus, the internal structure of the nodule preserves the original structure of the soil, even though it has been replaced by calcite. This replacive nodule growth (Colinson & Mountney, 2019) can be as well observed at the edges of the nodules where reaction rims show that the process of replacement has not reached completion (Figure 6 A, 6 B and 6 D). On the other hand, in rare cases, some nodules show evidence of displacive growth (Figures 5 E and 5 F). In this case during nodule growth host sediment is pushed aside and little or none is incorporated into within the nodule (Colinson & Mountney, 2019). Thus, displaced clay particles at the edge of the nodule prevent growth of calcite crystals in that direction, resulting in the formation of flat surfaces at the edge of nodule. (Figures 5 E and 5 F). It should be pointed out that although there is evidence of both, replacive and displacive growth of nodules, the replacive type of nodule growth is the dominant one, confirming *in situ* formation of these PC.

CONCLUSIONS

We studied a 0.95 m deep Calcocambisol soil profile located in the southeast part of the North Dalmatian Plain (Croatia). It consists of A-Bw-Bk-R mineral horizons, containing PC particles in deeper parts (> 23 cm). According to morphology (i.e. spherical to irregular in shape), these PC are classified as nodules. Microscopical analysis of these nodules showed that their formation takes place in situ, starting from multiple centres of nucleation, while inclusion of noncarbonate particles and preservation of the original soil structure confirms replacive nature of nodule growth. The final morphology and structure of a nodule is a result of multiple stages of precipitation and dissolution, indicating seasonal or event-based precipitation of carbonate.

ACKNOWLEDGEMENTS

Development Project-Training New Doctoral Students (DOK-2018-09-5748 and DOK-2021-02-1788) financed by Croatian Science Foundation. Currently, the contract of K.K. at USAL is financed by the European Union's Horizon 2020 research and innovation programme under the Marie Skłodowska-Curie grant agreement No. 101034371.

REFERENCES

Amit, R., Simhai, O., Ayalon, A., Enzel, Y., Matmon, A., Crouvi, O., Porat, N. & McDonald, E. (2011). Transition from arid to hyper-arid environment in the southern Levant deserts as recorded by early Pleistocene cummulic Aridisols. *Quaternary Science Reviews*, 30 (3-4). 312–323.

Barta, G. (2011). Secondary carbonates in loess-paleosoil sequences: A general review. *Central European Journal of Geosciences*, 3 (2). 129-146.

Bayat, O., Karimi, A., May, J.-H., Fattahi, M., Wiesenberg, G. L. B. & Egli, M. (2023). High-resolution record of stable isotopes in soil carbonates reveals environmental dynamics in an arid region (central Iran) during the last 32 ka. *Frontiers in Earth Science*, 11. 1-19.

Becze-Deàk, J., Langohr, R. & Verrecchia, E. P. (1997). Small scale secondary $CaCO_3$ accumulations in

selected sections of the European loess belt. Morphological forms and potential for paleoenvironmental reconstruction. *Geoderma*, 76 (3-4). 221–252.

Bensa, A., Švob, M., Domínguez-Villar, D., Perica, D. & Krklec, K. (2021). Parent material as a key determinant of sol properties in southern part of National park Krka, Croatia. *Agrofor International journal*, 6 (2). 116-123.

Bogunović, M., Bensa, A., Husnjak, S. & Miloš, B. (2009). Suitability of Dalmatian soils for olive tree cultivation. *Agronomski glasnik*, 71 (5-6). 367-404.

Borchardt, G. & Lienkaemper, J. J. (1999). Pedogenic calcite as evidence for an early Holocene dry period in the San Francisco Bay area, California. *GSA Bulletin*, 111 (6). 906–918.

Brlek, M. & Glumac, B. (2014). Stable isotopic ($\delta^{13}C$ and $\delta^{18}O$) signatures of biogenic calcretes marking discontinuity surfaces: a case study from Upper Cretaceous carbonates of central Dalmatia and eastern Istria, Croatia. *Facies*, 60 (3). 773-788.

Brlek, M., Korbar, T., Košir, A., Glumac, B., Grizelj, A. & Otoničar B. (2014). Discontinuity surfaces in Upper Cretaceous to Paleogene carbonates of central Dalmatia (Croatia): Glossifungites Ichnofacies, biogenic calcretes and stratigraphic implications. *Facies*, 60. 467–487.

Castellini, M., Stellacci, A. M., Tomaiuolo, M. & Barca, E. (2019). Spatial variability of soil physical and hydraulic properties in a durum wheat field: An assessment by the BEST-procedure. *Water*, 11 (10). 1434.

Chesworth W. (2008). *Encyclopedia of Soil Science*. Dordrecht, NL: Springer Dordrecht.

Čolak A. & Martinović J. (1973) Basic Soil Map of Croatia 1: 50 000 section Šibenik 1, Projektni savjet za izradu pedološke karte SRH, Split.

Colinson, J. D. & Mountney, N. P. (2019). *Sedimentary Structures*. Edinburgh, UK: Dunedin Academic Press Ltd.

Croatian Geological Institute (2009). *Geological map of Croatia M 1:300.000*. Zagreb, CRO: Croatian Geological Institute.

Danielson R. E. & Sutherland P. L. (1986). Porosity. In A. Klute (Ed.), *Methods of Soil Analysis: Part 1— Physical and Mineralogical Method* (pp. 443-461). New Jersey, U.S: John Wiley & Sons, Inc.

Domínguez-Villar, D., Bensa, A., Švob, M. & Krklec, K. (2022). Causes and implications of the seasonal dissolution and precipitation of pedogenic carbonates in soils of karst regions – A thermodynamic model approach. *Geoderma*, 423. 115962.

Driese, S. G. & Mora, C. I. (1993) Physico-chemical environment of pedogenic carbonate formation in Devonian vertic palaeosols, central Appalachians, USA. *Sedimentology*, 40 (2). 199-216.

Durand, N., Monger, H. C. & Canti, M. G. (2010). Calcium Carbonate Features. In G. Stoops, V. Marcelino & F. Mees (Eds.), *Interpretation of Micromorphological Features of Soils and Regoliths* (pp. 149–194). Elsevier Science.

Egli, M., Bösiger, M., Lamorski, K., Sławiński, C., Plötze, M., Wiesenberg, G.L.B., Tikhomirov, D., Musso, A., Hsu, S.-Y. & Raimondi, S. (2021). Pedogenesis and carbon sequestration in transformed agricultural soils of Sicily. *Geoderma*, 402. 115355.

FAO (2006). *Guidelines for Soil Description*, fourth ed. Rome, IT: FAO.

Filipčić, A. (1998). Climatic regionalization of Croatia according to W. Köppen for the standard period 1961–1990 in relation to the period 1931–1960. *Acta Geographica Croatica*, 33 (1). 1–15.

Fu, Y., Guo, Z. & Wang, G. (2023). Seasonality of C4 plant growth and carbonate precipitation in the Chinese Loess Plateau may cause positive carbon isotope anomalies in pedogenic carbonates. *Quaternary Research*, 120. 71–82.

Hakånsson, I. & Lipiec, J. (2000). A review of the uselfulness of the relative bulk density values in studies of soil structure and compaction. *Soil and Tillage Research*, 53 (2). 71-85.

Hasan, O., Miko, S., Ilijanić, N., Brunović, D., Dedić, Ž., Šparica Miko M. & Peh Z. (2020). Discrimination of topsoil environment in a karst landscape: an outcome of a geochemical mapping campaign. *Geochemical transactions*, 21 (1).

Hollis, J. M., Hannam, J., Bellamy & P. H. (2020). Empirically-derived pedotransfer functions for predicting bulk density in European soils. European *Journal of Soil Science* 63 (1). 96-109.

Husnjak, S. (2014) *Sistematika tala Hrvatske*. Zagreb, CRO: Hrvatska sveučilišna naklada.

ISO 10390:2005 (2005). Soil Quality - Determination of pH, Geneva: International Organization for Standardization.

ISO 10693:1995 (1995). Soil Quality - Determination of Carbonate Content, Volumetric Method, Geneva: International Organization for Standardization.

ISO 11272: 2017 (2017). Soil Quality – Determination of Dry Bulk Density, Geneva: International Organization for Standardization

ISO 11277:2009 (2009). Soil Quality - Determination of Particle Size Distribution in Mineral Soil Material. Method by Sieving and Sedimentation, Geneva: International Organization for Standardization

ISO 11461: 2001 (2001). Soil Quality - Determination of Soil Water Content as a Volume Fraction Using Coring Sleeves – Gravimetric Method, Geneva: International Organization for Standardization

ISO 11464:2006 (2006). Soil Quality - Pretreatment of Samples for Physico-Chemical Analysis, Geneva: International Organization for Standardization

ISO 11508:2017 (2017). Soil Quality – Determination of Particle Density, Geneva: International Organization for Standardization

Ivanović, A., Sikirica, V., Marković, S. & Sakač, K. (1977). *Osnovna geološka karta SFRJ 1:100 000, list Drniš K 33-9*, Institut za geološka istraživanja, Zagreb, Savezni geološki zavod, Beograd.

Ivanović, A., Sikirica, V. & Sakač, K. (1978). *Osnovna Geološka Karta SFRJ 1:100,000: Beograd, Tumač za List Drniš,* 59 p. Savezni geološki zavod.

JDPZ (1966) *Priručnik za ispitivanje zemljišta. Knjiga I. Kemijske metode ispitivanja zemljišta,* Beograd.

Jiménez-Ballesta, R., Bravo, S., Pérez-de-los-Reyes, C., Amorós J. A. & García-Navarro F. J. (2023).

Carbonate morphological features of vineyard soils in a semiarid Mediterranean environment. European *Journal of Soil Science*, 74 (6). e13435.

Krklec, K., Bočić, N., Perica, D. & Domínguez-Villar, D. (2024). Investigation of short-term denudation rates using the rock tablet method in Northern Velebit National Park (Croatia). *Hrvatski Geografski Glasnik - Croatian Geographical Bulletin*, 86 (1). 71-89.

Krklec, K., Domínguez-Villar, D., Carrasco, R. M. & Pedraza, J. (2016). Current denudation rates over a dolostone karst from central Spain: implications for the formation of unroofed caves. *Geomorphology*, 264. 1-11.

Krklec, K., Domínguez-Villar, D., Braucher, R., Perica, D., Mrak, I. & ASTERTeam (2018). Morphometric comparison of weathering features on side by side carbonate rock surfaces with different exposure ages - a case from the Croatian coast. *Quaternary International*, 494. 275-285.

Krklec, K., Domínguez-Villar, D. & Perica, D. (2021). Use of rock tablet method to measure rock weathering and landscape denudation. *Earth-Science Reviews* 212. 103449.

Krklec, K., Braucher, R., Perica, D. & Domínguez-Villar, D. (2022). Long-term denudation rate of karstic North Dalmatian Plain (Croatia) calculated from 36Cl cosmogenic nuclides. *Geomorphology*, 413. 108358.

Machette, M. N. (1985). Calcic soils of the southwestern United States. *GSA Special Papers*, 203. 1–22.

Mamužić, P. (1971). *Osnovna geološka karta SFRJ 1:100 000, list Šibenik, K 33-8*. Institut za geološka istraživanja, Zagreb, Savezni geološki zavod, Beograd.

Medak J. & Perić, S. (2007) Vegetation characteristics of Krka National Park. In D. Marguš (Ed.) *Book of Abstracts of the Symposium Krka River and Krka National Park: Natural and Cultural Heritage, Protection and Sustainable Development* (pp. 917-932). Šibenik, Croatia; Krka National Park.

Miloš, B. & Bensa, A. (2014). A GIS based assessment of agricultural resources for karstic areas of the Adriatic coastal region. *Agriculture and forestry*, 60 (4). 135-141.

Miloš, B. & Maleš, P. (1998). Soils of Kaštela bay and problems of their protection. *Agronomski glasnik*, 4. 185-204.

Monger, H. C. & Adams, H. P. (1996). Micromorphology of calcite-silica deposits, Yucca Mountain, Nevada. *Soil Science Society of America Journal*, 60 (2). 519-530.

Naiman, Z., Quade, J., Patchett & P. J. (2000). Isotopic evidence for eolian recycling of pedogenic carbonate and variations in carbonate dust sources throughout the southwest United States. *Geochimica et Cosmochimica Acta*, 64 (18). 3099-3109.

Panagos, P., Meusburger, K., Ballabio, C., Borrelli, P. & Alewell, C. (2014). Soil erodibility in Europe: A high-resolution dataset based on LUCAS. *Science of the Total Environment*, 479–480. 189–200.

Pilaš, I., Medak, J., Vrbek, B., Medved, I., Cindrić, K., Gajić-Čapka, M., Perčec Tadić, M., Patarčić, M., Branković, Č. & Güttler, I. (2016). Climate Variability, Soil, and Forest Ecosystem Diversity of the Dinaric Mountains. In G. Zhelezov (Ed.), *Sustainable Development in Mountain Regions* (pp. 113-139). Dordrecht, NL: Springer Dordrecht

Rabenhorst, M. C. & Wilding, L. P. (1986). Pedogenesis on the Edwards Plateau, Texas: III. New model for the formation of petrocalcic horizons. *Soil Science Society of America Journal*, 50 (3). 693-699.

Rovira, P. & Vallejo, V. R. (2008). Changes in δ13C composition of soil carbonates driven by organic matter decomposition in a Mediterranean climate: A field incubation experiment. *Geoderma,* 144 (3–4). 517-534.

Royer, D.L. (1999). Depth to pedogenic carbonate horizon as a paleoprecipitation indicator? *Geology*, 27 (12). 1123–1126.

Škorić, A., Filpovski, G. & Ćirić, M. (1985). *Soil classification of Yugoslavia*. Sarajevo, B&H: Academy of Sciences of Bosnia and Herzegovina.

Sobecki, T. M. & Wilding, L. P. (1983). Formation of calcic and argillic horizons in selected soils of the Texas Coast Prairie. *Soil Science Society of America Journal*, 47 (4). 707–715.

Stoops, G. (2003) *Thin section preparation of soils and sediments. Madison*, USA: Soil Science Society of America, Inc.

Švob, M., Bensa A., Domínguez-Villar, D., Perica, D. & Krklec, K. (2021). Basic properties of Calcocambisol from a location on North Dalmatian plain. *Agriculturae Conspectus Scientificus* 86 (4). 305-316.

Velić, I., Vlahović, I., (2009). *Tumač Geološke karte Republike Hrvatske 1:300000*. Zagreb, Croatia: Hrvatski geološki institut

Verrecchia, E. P. & Trombino, L. (2021). *A Visual Atlas for Soil Micromorphologists*. Dordrecht, NL: Springer Dordrecht.

Vrbek B. & Pilaš I. (2007a). Soils of Krka National Park. In D. Marguš (Ed.), *Book of Abstracts of the Symposium Krka River and Krka National Park: Natural and Cultural heritage, Protection and Sustainable Development* (pp. 949-977). Šibenik, Croatia: Krka National Park.

Vrbek, B. & Pilaš, I. (2007b). Contribution on knowledge of Štirovača soils on Velebit, *Radovi – Šumarski institut Jastrebarsko*, 42 (2). 155-166.

Wagner, S., Günster, N. & Skowronek, A. (2012). Genesis and climatic interpretation of paleosols and calcretes in a plio-pleistocene alluvial fan of the costa blanca (SE Spain). *Quaternary International*, 265. 170-178.

West, L. T., Wilding, L. P. & Hallmark, C. T. (1988). Calciustolls in Central Texas: II. Genesis of Calcic and Petrocalcic Horizons. *Soil Science Society of America Journal*, 52 (6). 1731-1740.

Wieder, M. & Yaalon, D. H. (1982). Micromorphological fabrics and developmental stages of carbonate nodular forms related to soil characteristics. *Geoderma*, 28 (3-4). 203–220.

Zamanian, K., Pustovoytov, K. & Kuzyakov, Y. (2016). Pedogenic carbonates: Forms and formation processes. *Earth-Science Reviews*, 157. 1-17.